Journal of Thermal Analysis and Calorimetry
https://doi.org/10.1007/s10973-021-10800-8

Numerical optimization of a conical cavity as a radiation-focused concentrator

Ali Heydari[1] · Mehrdad Mesgarpour[2] · Somchai Wongwises[2,3]

Received: 20 November 2020 / Accepted: 29 March 2021

Abstract

Conical enclosures rely on the conical cavity and can be used as radiation concentrators. Two circular cross-section baffles were used to improve the heat transfer of this geometry. By changing the rigid fins to porous, it could improve the heat transfer. Al_2O_3/water nanofluid was also employed to enhance the heat transfer performance of the cavity. For this purpose, numerical analysis of three-dimensional natural convection heat transfer was performed in a conical cavity with two types of fins. The best combination of fins arrangement for the next step was selected using the differential evolutionary optimization method (D.E). In this case study, a new combination of laminar and turbulence methods was employed for the first time to increase the accuracy of the natural convection solution. This combination is based on the laminar solution by suppressing the perturbation parameter in the turbulence method which led to more accurate results. The analysis results showed that a conical cavity with optimized fin geometry can lead to a 23% increase in Nu. The best porosity for the inner fin was calculated 40% in the case of constant porosity. Ascending porosity along the fin, whose increase was more intense near the base and slower near the cone's tip, was the best variable porosity for the inner fin.

Keywords Conical cavity · Porous fin · Radiation concentrator · Natural convection · Nanofluid · Optimization

Nomenclature

A	Surface area (m^2)
C_p	Specific heat (J kg^{-1} K^{-1})
$C_{1\varepsilon}$ $C_{2\varepsilon}$,$C_{3\varepsilon}$	Constant
Ef	Effectiveness
Gr	Grashof number
G_k	Turbulence kinetic energy production in terms of velocity gradient (J)
G_b	Turbulence kinetic energy production in terms of buoyancy force (J)
g	Gravity (m s^{-2})
h	Convection heat transfer coefficient (W m^{-2} K^{-1})
K	Thermal conductivity (W m^{-1} K^{-1})
k	Kinetic energy (J)
L	Length (m)
L_c	Characteristic length (m)
Nu	Nusselt number
P	Pressure (Pa)
Pr	Prandtl number
Q	Heat transfer rate (W)
Ra	Rayleigh number
Re	Reynolds number
S	Motion source term
S_K S_ε,	Source terms
t	Time (s)
T	Temperature (K)
u_i	Velocity component (m s^{-1})
U	Velocity vector (m s^{-1})
$\hat{e}_z$	The unit vector in the upward vertical direction
U_i^*	Dimensionless velocity component
$Y_{.M.}$	Oscillation share in the turbulence density
x_i	Direction component

Greek symbols

α	Thermal diffusivity (m^2 s^{-1})
β	Thermal expansion (K^{-1})
κ	Medium permeability

✉ Mehrdad Mesgarpour
mehrdad.mes@kmutt.ac.th

[1] Department of Mechanical Engineering, University of Torbat Heydarieh, Torbat Heydarieh, Iran

[2] Fluid Mechanics, Thermal Engineering and Multiphase Flow Research Lab. (FUTURE), Department of Mechanical Engineering, King Mongkut's University of Technology Thonburi (KMUTT), Bangmod, Bangkok 10140, Thailand

[3] National Science and Technology Development Agency (NSTDA), Pathum Thani 12120, Thailand

Published online: 12 May 2021

ε	Dissipations rate
η	Efficiency
θ	Non dimensional temperature
μ	Dynamic viscosity (Pa s)
ρ	Density (kg m^{-3})
τ	Tension (N m^{-2})
υ	Kinematic viscosity (m^2 s^{-1})
φ	Volume fraction

subscripts

ave	Average
b	Base
c	Cross section
cond	Conduction
conv	Convection
f	Fluid
fin	Related to fin
in	Inlet
i, j	Components
out	Outlet
s	Solid
t^*	Turbulence
total	Total
∞	Ambient

Introduction

Natural convection heat transfer in close enclosures could be exploited to store and transfer heat in various furnaces, cooling electronic components, heat exchangers, cooling and heating of buildings, and solar technologies. One of the most critical natural convection heat transfer applications in the conical cavities is their use as a point-focused solar concentrator system. Increasing heat transfer in these enclosures can improve the performance of the solar system. In these systems, The pumped fluid transfers thermal energy to the heat receiver, which supplies it to the system [1].

The cavity receiver type is one type of thermal receivers which has been studied in different geometries, dimensions, and positions for diverse applications. For example, Reddy et al. [2] studied the all method in heat transfer (radiation, natural, and forced convection) heat losses of a hemispherical cavity receiver in terms of various factors. Their results indicated the minimum natural convection heat loss at the receiver's open side faced downwards. Moreover, they proposed a correlation between the radiation Nusselt number(Nu) and the convection heat transfer losses. Prakash [3] numerically investigated the natural convection heat losses of cylindrical close enclosure receivers with different diameters. The model simulated the flow inside a helical coil with air as the heat transfer working fluid.The result indicated that the decrease in the convection heat transfer loss is due to the enhancement in the receiver inclination, while the increase in the convection heat transfer losses can be assigned to the rise in the mean temperature of the heat transfer fluid (HTF) and the opening ratio. In a numerical study, Si-Quan et al. [4] studied the optical and thermal performance of a spherical close enclosure receiver using the Monte-Carlo Ray Tracing Method and CFD model. They found that the spherical close enclosure receiver had better performance than other receivers. They also investigated the effect of inlet temperature and velocity on three types of heat losses. The performance of a novel cavity receiver was analyzed for application in parabolic through solar collectors in the work by Liang et al. [5] who experimentally and theoretically explored the effects of physical parameters on the thermal performance of the cavity. Their results indicated that the collector efficiency could reach 64.25% under optimal conditions. Al-Kouz et al. [6] numerically assessed the two-dimensional natural convection heat transfer in a close enclosure with two rigid fins attached to the hot wall. They found that attaching two rigid fins to the hot wall would increase the heat transfer for such flows and enhance the length of the fin, giving rise to a better heat transfer. In another study on a cavity with fins, Ngo et al. [7] numerically analyzed simultaneous natural convection and radiation heat transfer in a solar cavity receiver. According to their results, the use of the plate fins reduced the radiation and natural convection heat losses by 5% and 20%, respectively, while causing a 2% increase in overall cavity efficiency.

One way to control heat transfer in close enclosures is to use porous expanded surfaces which can increase or decrease heat transfer rate in a specific state by creating obstacles to control vortexes. In this regard, numerous studies have addressed the heat transfer in enclosures with porous fins. For example, Khanafer et al. [8] numerically studied natural convection in a square cavity with a thin porous fin attached to the hot wall. Their results indicated that using a porous fin increased the average Nu when it was placed either close to the bottom or in the middle of the vertical surface at an angle of 90°. In another numerical study, Siavashi et al. [9] evaluated entropy generation and natural convection of flow inside a cavity using nanofluid and porous fins. According to their results, adding porous fins with a high Da improved heat transfer, while fins with a small Da led to a reduction in Nu due to weakening the convection.

Alshuraiaan and Khanafer [10] analyzed the laminar natural convection heat transfer in a heated cavity along with the heated thin porous fin. Their results specified that using a horizontal porous fin increased the Nu while a vertical fin attached to the bottom led to a lower Nu than without fins. Asl et al. [11] comprehensively investigated the influence of

solid and porous fins in an inclined rectangular enclosure. They showed that the use of the conductive porous fins in the enclosure resulted in 41% heat transfer enhancement as compared with enclosures having solid fins and up to 20% compared to cavities without fins. Their results also indicated that optimum porous fin length was a decreasing function of the Ra. Mesgarpour et al. [12, 13] numerically and experimentally assessed the natural convection in an enclosure with an engineered hot porous plate at different positioning angles and revealed that the best positioning angle to reach the highest Nu in the enclosure is 45°. They also stated a correlation between the Nu and the Ra.

Specifically, the application of cavity enclosures in radiation-focused systems has been also studied. In a numerical study, Daabo et al. [14] addressed the optical efficiency and thermal behavior of three different geometries of a cavity receiver in the concentrated solar applications. Based on their findings, the conical receiver offered a lower heat loss while absorbing a higher amount of reflected energy. Pe´rez-Ra´bago [15] experimentally and numerically investigated heat transfer in a conical cavity calorimeter to calculate the thermal power of solar concentrator. They calculated the efficiency of the device which can be useful in the optimized design of the calorimeter. Garrido et al. [16] analyzed the performance of a Dish-Stirling cavity receiver in different geometries and operating temperatures both experimentally and numerically. It was found that the reverse-conical cavity was more efficient than a nearly cylindrical shape. The latest papers on the cavity are presented in Table 1.

The applications of nanofluids in cavities have been investigated by numerous researchers. A nanofluid is a fluid (water, ethylene glycol, and oil) in which nanoparticles are suspended. Nanofluids can increase heat transfer by higher thermal conductivity compared with the base fluid. Numerous studies have been devoted to predicting and evaluating the thermal conductivity of nanofluids [27–29]. Rostami et al. [30] presented a review on experimental and numerical studies about different shapes of nanofluid-containing cavities and determined effective parameters in the natural convection of these cavities. Their results showed that natural convection in cavities depends more on the induced fluid velocity due to the forced convection, which can be increased by nanoparticle addition, magnetic fields, fins, and porous media. Ho et al. [31] explored the sedimentation of Al_2O_3/water nanofluids in a rectangular cavity applying Ludwig–Soret effect, Brownian motion and sedimentation in the numerical analysis. Their results well agreed with experimental findings. In a numerical study, Safaei et al. [32] used the *lattice Boltzmann method (LBM)* to analyze the interaction between thermal radiation and natural convection in a 2D shallow cavity filled with Al_2O_3/water nanofluid. They declared that the total Nu number is enhanced for higher Rayleigh number and emissivity, implying that thermal radiation combined with natural convection heat transfer might increase the Nusselt number. Goodarzi et al. [33] numerically simulated a 2D rectangular cavity with different aspect ratios using hybrid nanofluid (Cu-multi-walled carbon nanotubes- Al_2O_3). They indicated that fluid circulation due to natural convection leads to heat transfer in the cavity. In another numerical simulation, Abbassi et al. [34] studied natural convection in an incinerator with a hot block filled with nanofluid considering magnetohydrodynamics (MHD) using LBM. They concluded that entropy generation is increased by augmenting the height and width of the heater, the volume fraction of nanoparticles, and the Rayleigh number. It, however, decreased by increasing the Hartmann number. To improve heat transfer, the optimum incinerator inclination angles was obtained 90°. Kolsi et al. [35] analyzed the convection in a 3D open cavity containing a diamond-shaped obstacle surrounded by Al_2O_3/water nanofluid. They investigated the effect of volume fraction,

Table 1 Review of the latest papers on the cavity

No.	Base fluid	Additive	Cavity type	Ra range	Method	Solver	Nu range	Refs.
1	Water	AL_2O_3 solid nanoparticle	Square porous	10^6	Finite difference method	CFD code	0–16	[17]
2	Casson fluid	-	Square porous	10^2–10^6	Finite element	CFD code	0–15	[18]
3	Water	CNT	Square	10^3–10^6	Experiment	–	0–20	[19]
4	Water	Cu nanofluid	Wavy	10^3–10^6	CVFEM	CFD code	0–8.7	[20]
5	Water	Cu nanofluid	Triangular	0–10^5	CVFEM	CFD code	0–9	[21]
6	Water	(MWCNT)-Fe_3O_4	P-shaped	10^3–10^4	Lattice Boltzmann	–	0–2.89	[22]
7	Water	(MWCNT)-Fe_3O_4	T-joint	10^3–10^6	FVM	CFD code	12–24	[23]
8	Water	Cu–Al_2O_3	Square	10^6–10^8	FVM	CFD code	0–62	[24]
9	Water	Ag–MgO	Square	10^4–10^5	PDEs	–	0.25–3.8	[25]
10	Non-Newtonian	–	U-shaped	10^6	PARDISO	CFD code	0–13	[26]

Rayleigh number and width of diamond shape and indicated that the partition geometry could control the heat and fluid flow inside the cavity. In another related numerical investigation, Yousefzadeh et al. [36] simulated laminar mixed convection heat transfer inside a square cavity with different heat transfer areas with a hot isothermal circular heat source at the middle of the cavity. They used silver/water nanofluid and showed smaller temperature gradients near the hot surface due to the increase in Reynolds number. Uniform temperature distribution can be achieved when the heat transfer area is placed in a suitable location. Pordanjani et al. [37] considered magnetic field and thermal radiation to study the free convection and entropy generation in a diagonal rectangular cavity filled with nanofluid. An increase in Nusselt number and entropy generation and a decrease in Bejan number were observed by enhancing Rayleigh number and reducing the Hartmann number. Overall, nanofluids has been used in many heat transfer applications related to solar energy [38–40]. Optimization process can improve efficiency and heat transfer. It can also modify the geometry and shape [41].

According to studies in heat transfer of cavities, the conical cavities, especially with porous fins, have been less analyzed. In addition to investigating the thermal performance of a conical cavity in the present work, its optimization is addressed by nanofluids and porous fins, which is the first work in this field. Thus, in this paper, a numerical study was performed to investigate the heat transfer performance of a conical cavity with two cylindrical engineered porous fins attached to the hot base surface. The effects fin spacing, their height ratio, and their porosity were examined on the thermal performance of the cavity. The study of the 3D geometry of the conical cavity under natural convection heat transfer is entirely different from the regular square cavity. In this case study, non-symmetric natural convection flow was also reviewed. The typical optimization process of geometry is usually limited to RSM and Genetic methods. The D.E process is based on parameter prediction; therefore, this process is much accurate and suitable for geometry optimization.

Problem definition and boundary conditions

To model the natural convection and study the effect of geometry on heat transfer, a three-dimensional conical cavity was investigated with cylindrical porous obstacles at different distances, heights and porosities. Figure 1 shows the conical enclosure with obstacles with various heights and distances. In this case, [A] varied between 0 and 6.5 cm, [B] varied between 7.5 cm and 9.5 cm and [L] changed between 2 and 13 cm. These ranges were selected based on assumptions and geometrical restrictions. It was assumed that 50% of the base surface is dedicated to each fin and the minimum space between fins is 1 cm. The height of baffle 1 was considered fixed. After finding the optimal distance and the best height of the inner fin, the effect of porosity was examined for 8 different porosity percentages (0–70%).

The bottom hot plate transfers the Al_2O_3/water nanofluid upwards at $\varphi = 1\%$, and the cold side plates cools it down. The internal fins and the cavity frame are made of copper, to enhance the heat transfer. Figure 1 shows that the fins are concentric cylinders. Boundary conditions of the problems are indicated in Table 2.

Table 2 Boundary conditions and initial value

Location	Boundary condition	value	Unit
Hot side	Heat flux	800	Wm^{-2}
Cold side	Constant temperature	25	°C
Baffle	Wall	–	–

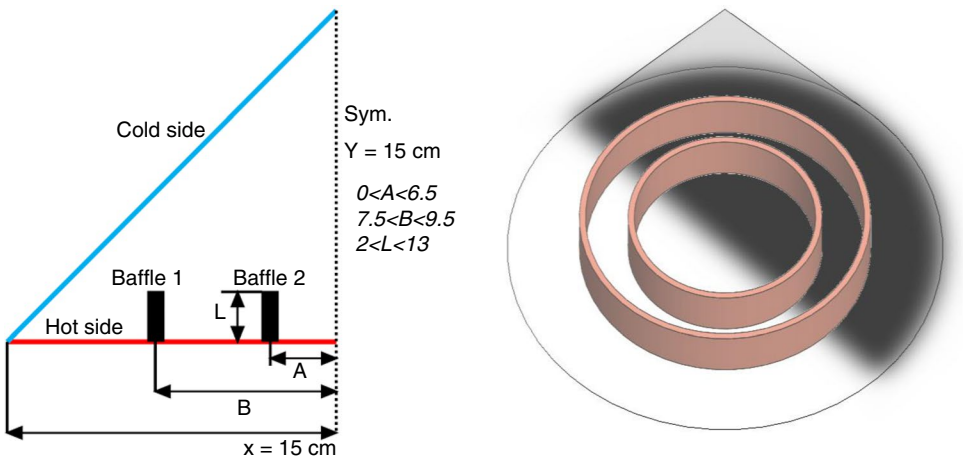

Fig. 1 Geometrical properties of the cavity and fins, dimensions (left) and position of fins(right)

In this case study, a specific code was generated in Python software for modeling natural convection in the cavity. For the optimization section, the D.E algorithm was added to the base code. The Boussinesq approximation was used to model natural convection. PISO algorithm was also used for pressure–velocity coupling. All equations were in the second order of accuracy. The grid generation code generates a thorough structure inflation grid, and curvature correction was used for a corner. To model this simulation, 16 GB RAM and 23 cores of CPU were used. All the results were plotted in origin software.

Governing equations

At the representative elementary volume (REV), Darcy's law for fluid flow in the pore space is as follows [13]:

$$u = \frac{k}{\mu}\nabla P \tag{1}$$

where, u is the velocity of fluid and P is pressure of fluid at the pore scale. The κ represents the medium permeability, and μ is the dynamic viscosity.

Boussinesq equations in this case study are according to [42]:

$$\frac{\partial v}{\partial t} + (v.\nabla)v = -\nabla p + \Pr\nabla^2 + Ra\Pr T\hat{e}_z \tag{2}$$

$$v.\nabla = 0 \tag{3}$$

$$\frac{\partial T}{\partial t} + (v.\nabla)T = \nabla^2 T \tag{4}$$

In this equation, the velocity v and T is the fluid temperature. Due to low temperatures in the fins (in this problem), the radiation can be ignored in porous fins [43]. According to the energy balance in a control volume of the internal fin inside the conical cavity, regardless of radiation heat transfer, we have:

$$\dot{Q}_{\text{total}} = \dot{Q}_{\text{cond}} + \dot{Q}_{\text{conv}} \tag{5}$$

In the above expression, $\dot{Q}_{\text{cond}}$ and $\dot{Q}_{\text{conv}}$ are the heat transfer rate by conduction and convection, respectively, for which we have:

$$\dot{Q}_{\text{cond}} = K_{\text{fin}}A_c\frac{\partial T}{\partial x} \tag{6}$$

$$\dot{Q}_{\text{conv}} = hA_s\left(T_s - T_\infty\right) \tag{7}$$

where h is the natural convection heat transfer coefficient, T_s and T_∞ are the temperatures of surface and ambient, respectively, A_c and A_s are the solid cross-section and solid surrounding surface area, respectively. K_{fin} is the thermal conductivity of the fin.

For Nu and Ra based on characteristic length (L_c) are as follows:

$$Nu_L = \frac{h_{av}L_c}{K_f}, Ra_L = \frac{g\beta\left(T_s - T_\infty\right)L_c^3}{\nu\alpha} \tag{8}$$

The average convection heat transfer coefficient (h_{av}) of the cavity in Eq. (7) can be obtained as follows:

$$h_{av} = \left(\frac{\dot{Q}_{\text{conv}}}{A_s\left[T_s - T_\infty\right]}\right) \tag{9}$$

where, T_s is the temperature of the hot surface, T_∞ is the ambient fluid temperature (which was averaged in 10 lines in the cavity) and A_s is the lateral surface of the hot plate. The thermal efficiency (η) and effectiveness (Ef) of the fin can be calculated from: [12, 44].

$$\eta_{\text{fin}} = \frac{Q_b}{h_{\text{fin}}A_s\left(T_b - T_\infty\right)} \tag{10}$$

$$Ef = \frac{Q_b}{h_{\text{fin}}A_c\left(T_b - T_\infty\right)} \tag{11}$$

where h_{fin} is convection heat transfer coefficient around the fin surface in the natural convection. It must be noted that the estimation way of heat transfer coefficient for the cavity and the fin in Eqs. (6) and (7) is different because of the different lateral surfaces.

Turbulent model

The typical laminar viscous model was employed to model the natural convection. When the natural convection was selected, some critical details of the simulation such as the vortex and dissipation rate will be lost. In this case, for the first time, a combination of the laminar and turbulent method was used to increase the accuracy and address the effect of geometry on heat transfer and fluid flow in the conical cavity. This combination is based on the *laminar* solution by suppressing the perturbation parameter in the turbulence method. Some novel correlations were used to transform the laminar model to turbulence. The range of Re for this transform was 0.00025–0.00741. The turbulence in this

simulation was the k-ε model. The equations for kinetic energy of turbulence (k) and dissipations rate (ε) are as follows [45]

$$\frac{\partial}{\partial x_i}(\rho k u_i) + \frac{\partial}{\partial t}(\rho k) = \frac{\partial}{\partial x_j}\left(\left(\mu + \frac{\mu_{t^*}}{\sigma_k}\right)\frac{\partial k}{\partial x_j}\right) + G_K + G_b - \rho\varepsilon - Y_M + S_K \tag{12}$$

$$\frac{\partial}{\partial x_i}(\rho \varepsilon u_i) + \frac{\partial}{\partial t}(\rho \varepsilon) = \frac{\partial}{\partial x_j}\left(\left(\mu + \frac{\mu_{t^*}}{\sigma_\varepsilon}\right)\frac{\partial \varepsilon}{\partial x_j}\right) + C_{1\varepsilon}\frac{\varepsilon}{k}(G_K + C_{3\varepsilon}G_b) + C_{2\varepsilon}\rho\frac{\varepsilon^2}{k} + S_\varepsilon \tag{13}$$

where, G_K is the production of turbulence kinetic energy, G_b is turbulence kinetic energy from buoyancy forces and Y_M is the oscillation contribution in the turbulence density to the total loss. $C_{1\varepsilon}$, $C_{2\varepsilon}$ and $C_{3\varepsilon}$ are constant and S_K and S_ε denote the source terms [45].

Nanofluid properties

Thermal conductivity and viscosity are temperature dependent and specific for each nanofluid. To improve the accuracy, the thermal conductivity was calculated from an individual correlation temperature-based $\varphi = 1\%$. The correlations for thermal conductivity and viscosity are shown in Table 3. The correlation of thermal conductivity is extrapolated from diagrams in the related references.

In this case study, the important assumptions are:

1. Constant heat flux is provided.
2. Conduction heat transfer in the fin is only function of heat transfer inside the cavity.
3. The conduction and convection boundary condition on the fin surface are solve coupled in constant time step.
4. The convection boundary condition in the cavity are solved in both transient and steady state.
5. Low-temperature surface on the side was consider at a constant temperature.
6. The numerical analysis was performed for axisymmetric 3D configuration, and the vertical side was defined as the axis boundary condition.

There are two important reasons for selecting this type of nanofluid of AL_2O_3. First, this type of nanofluid has been intensively explored. In this simulation, the thermal conductivity and viscosity of AL_2O_3 nanofluid are temperature dependent; thus, it is vital to know the behavior of nanofluids in the range of operation temperature. The correlations in Table 3 have a good adaptation with an experimental test. The second reason refers to the algorithm of simulation. For the first time in this code, both types of viscosity model (laminar and turbulence) were simultaneously included to increase heat transfer. This is NOT just a solution; as this method can increase the accuracy as well. AL_2O_3 nanofluid has been experimentally and numerically investigated in a wide range of Nu and Ra. To simulate, a constant parameter in the Navier Stocks equation is required. In commercial software such as fluent and CFX, this constant parameter is set to its default value. In this code, this constant parameter was directly extracted from the experimental results.

Geometric optimization

One of the fundamental imperfection of optimization methods is that they present a local optimum instead of a overall one. Genetic and differential evolution method are evolutionary optimization algorithms [41, 50, 51] that were matured for recommendation the overall optimum of the optimization case studies. D.E. is a relatively unique evolutionary optimization algorithm. It is a population-based optimization method introduced by Price et al. [52] who matured a offbeat booming, versatile, and easy-to-use overall optimization algorithm. This algorithm is indicated in Fig. 2.

Mesh study and validation

Regarding the inherent error in any numerical solution, validation and network analysis are the two most critical

Table 3 Correlations for thermal conductivity and viscosity

Nanofluid property	Equation	Restrictions	Ref
Thermal conductivity	$k(T) = (0.261 - 0.00417T)^{-0.033}, R^2 = 0.9868$	$\varphi = 1\%$ $290K < T < 340K$	[46, 47]
Viscosity	$\mu_r = 1.125 - 0.0007T$	$290K < T < 340K$ $1\% \le \varphi \le 4\%$	[48, 49]

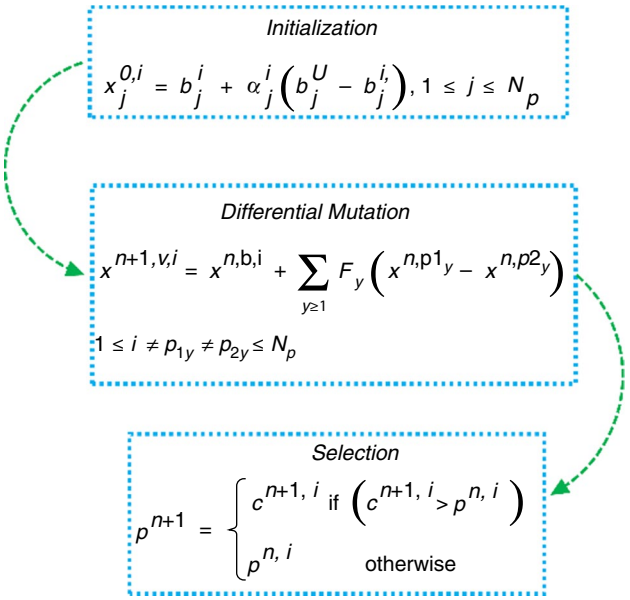

Fig. 2 Algorithm of differential evaluation (D.E)

issues to be examined. All calculations were performed on the produced domain on the fluid and body regions. By changing the mesh number, the computational volume also varies, which significantly affects the final results. On the other hand, as the number of computing grids increases, the computational time will be enhanced. In other words, each numerical analysis is a specific function of the mesh size value in which the lowest computational cost and the highest analysis accuracy are achieved. In this case study, due to grid generation on the conical cavity and creating the calculation domain on the conical cavity, a unique code was added to the original code. There are 2 essential topics in grid generation in this case study. First, in natural convection, the gradient of velocity is shallow. Therefore, any inequality can increase the error. The second issue is the corner. In this geometry, the corner has a sharp edge and its refinement in the grid is essential. According to Fig. 3a, a mesh study was performed for two Nu and mean temperature parameters of the conical cavity. The results clearly suggest that by increasing the number of network grids, two parameters in a certain number reach their final level of change. Another critical issue in examining mesh independence in this work is the geometric change during the optimization. The variation of y^+ base of several grids is presented in Fig. 3b. Since the use of the optimization algorithm changes the geometry, the mesh independence should be examined for each analysis range. According to the geometric characteristics of the problem and the use of aluminum dioxide nanofluid with a specific volume fraction and porous fins, the issues under validation are divided into two modes. For comparing CFD and reference papers, variation in Nu with different Ra was examined for one case as a porous triangle cavity with nanofluid [19] and another case was a non-porous triangle cavity with nanofluid [20]. Figure 4 compares CFD results and Chowdhury et al. [53] report for a triangular cavity with and without porous media. Accordingly, it can be concluded that the maximum deviation of CFD results and reference was 6.67% confirming the accuracy of the results. In this

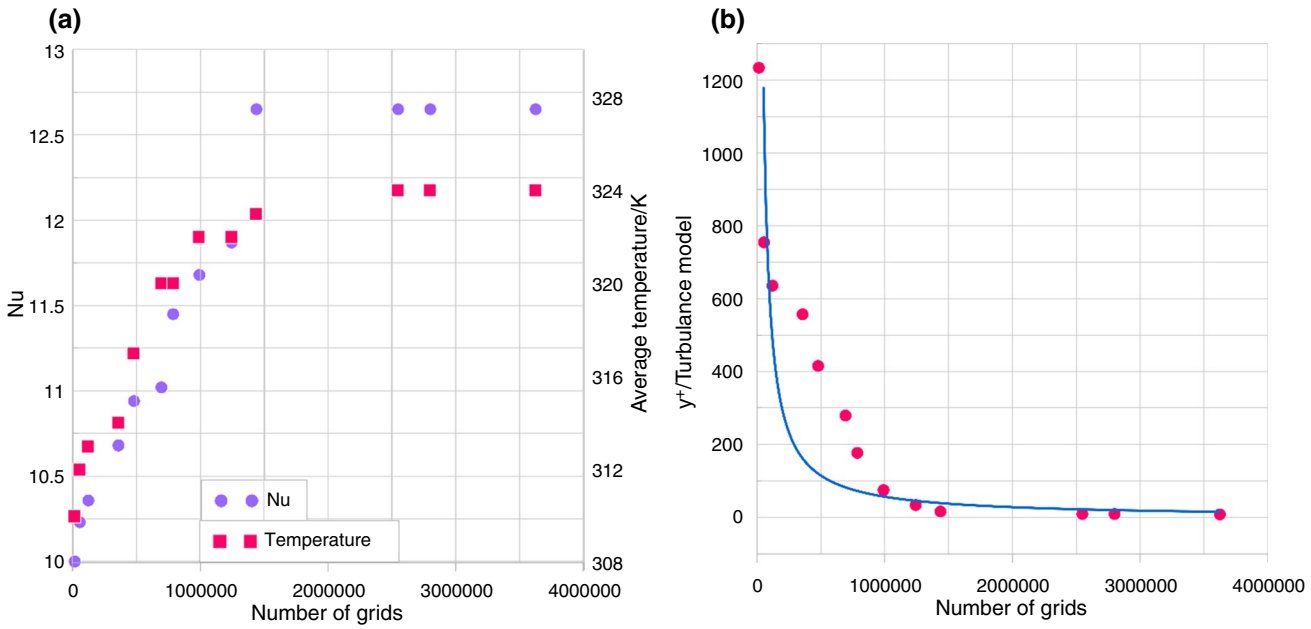

Fig. 3 Grid study for (**a**) Nu and average temperature and (**b**) variation of y^+

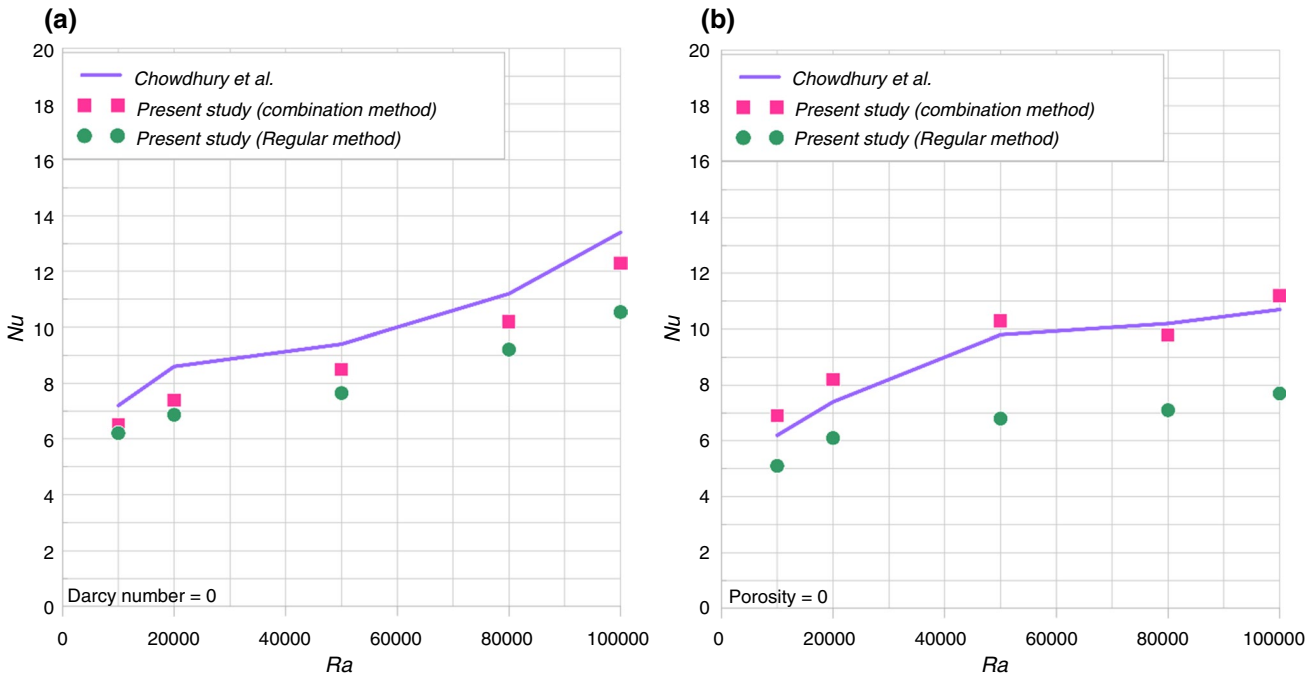

Fig. 4 Validation of CFD results and reference papers for a triangular enclosure (**a**) Chowdhury et al. [53] in Da = 0 and **b** Chowdhury et al. [53] in porosity = 0

Fig, a comparison is also made between the combination method (laminar and turbulence) and the traditional method (fully laminar). The result indicated that the combination method can improve the accuracy.

Result and discussion

Natural convection heat transfer has been extensively researched due to its wide application in heat transfer. The Boussinesq equations, as the basis of the momentum equation, create a flow inside the cavity. The three-dimensional structure of the problem allows studying the detail of the problem. Density changes along the cone height are essential factors in heat transfer from the hot plate to the cold one. Internal circular barriers affect the overall heat transfer by two conduction mechanisms: heat transfer and change in the flow regime.

The first step in any numerical optimization is to study the sensitivity analysis of the parameters. Sensitivity analysis is a statistical method to measure the impact of each independent parameter on a unique final solution. In other words, by performing sensitivity analysis for independent variables, it is possible to find the priority of each variable over the results. In this case, the useful parameters in optimization are the fin spacing and their height. The sensitivity of three main independent parameters of the problem to the Nu was evaluated. Figure 5 shows that the fins (L) height significantly affects the Nu. Also, after height, the distance of the internal obstacle (A) and then the distance of the external obstacle (B) have the most significant effects on the Nu. Another significant result of this diagram is that the most considerable amount of Nu can be generated at specific values of each presented parameter. In other words, sensitivity analysis reduces the amount of data to be used in the optimization process. This helps to focus on optimal values in addition to increasing the solution speed.

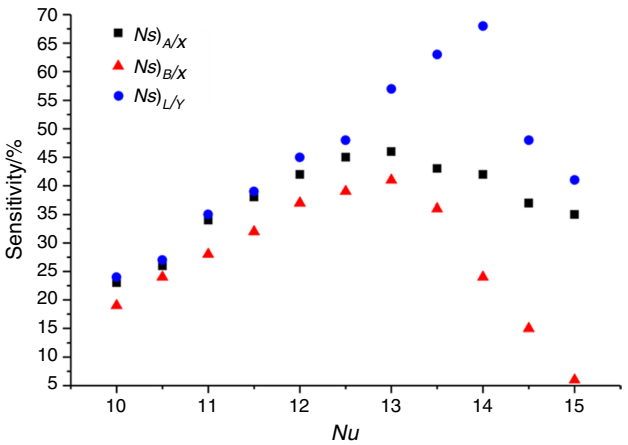

Fig. 5 Sensitivity analysis for the effect of variable parameters on Nu

Optimization

One of the limitations of numerical simulation is the range of modeling the parameters in every simulation. In other words, each analysis can be only applied for one geometry or boundary condition. The numerical solution has a unique and specific answer to its specific geometry and boundary condition. In this section, using optimization methods, it is tried to find the most influential parameter on the heat transfer to determine the changes of the Nu due to variation in these parameters. In all geometries, the heat was transferred from the hot plate (bottom plate) to the fluid through circular fins. The fins were placed at the bottom of the cavity and could affect the heat transfer rate from the base. These fins incremented the area of the hot surface. Secondly, they will alter the flow pattern inside the conical cavity due to their rigid structures. An increase in the number and intensity of the vortices will increment the net amount of heat transfer. As mentioned in the previous sections, two ring-shaped fins were used in this cavity. The effect of their distance from the center of the cavity was investigated. The height of fins was assumed to be constant. After estimating the optimum distances, the height of the internal fin changes for fixed optimum distances in the next step. Figure 6 a presents the effect of changes in the distance between the inner fin and the center of the cavity ($^{A}/_{X}$) on the Nu, efficiency and effectiveness of the fin, and the average temperature. The results clearly show that an increase in the distance between the inner fin and the cavity center will first augment the average temperature followed by a decrease after (A/X > 0.3). In other words, the average temperature at a point reaches its maximum value. Consequently, the Nu was close to its highest value in proportion to the average temperature (Fig. 6a). Similarly, in Fig. 6b the efficiency and effectiveness increased and decreased before and after maximum value, respectively. The results show that $^{A}/_{X} \cong 0.3$ leads to the highest efficiency and effectiveness of a conical cavity above which, the efficiency and effectiveness dramatically reduced. The exact optimum values of the $^{A}/_{X}$ for efficiency and effectiveness are 0.32 and 0.27, respectively.

Since efficiency and effectiveness are different in terms of the surface area changes, the lateral surface area and fin base surface based on the distance between the inner fin and the center of the cavity can play an influential role in explaining the efficiency and effectiveness. Another parameter studied in this research was the distance of the external fin to the center of the cavity ($^{B}/_{X}$). Figure 7 shows that the average temperature of the conical cavity increased and then sharply decreased upon enhancing $^{B}/_{X}$. One of the crucial issues in temperature distribution within a conical cavity is the amount and intensity of vortices. The external fin was located in the outer region where the cold wall is lower, making it possible to form many inactive (useless) vortices. Figure 7a indicates that after a certain distance, the average temperature rapidly reduced with $^{B}/_{X}$ increment. The maximum range of the Nu also varies with average temperature. According to part (b) of Fig. 7, the maximum efficiency and effectiveness for fins occurred at $^{B}/_{X}$ equal to 0.59 and 0.58, respectively.

Figure 8 illustrates the effect of dimensionless height of the inner fin ($^{L}/_{Y}$) on the Nu, the average temperature, efficiency, and effectiveness of the fin. An increase in the height of the inner fin augmented the average temperature followed

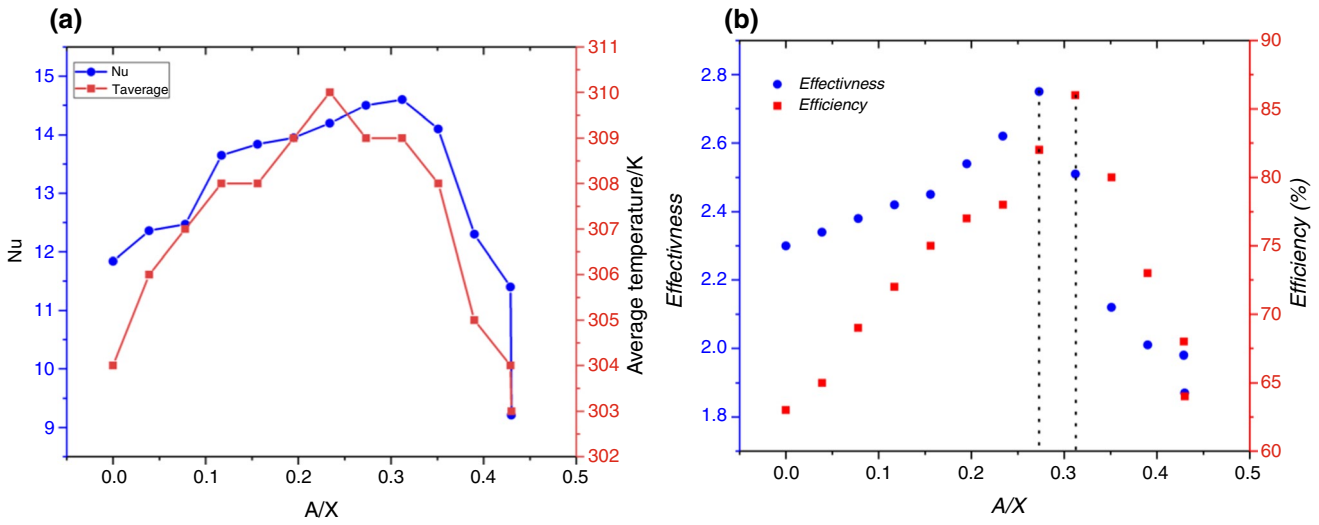

Fig. 6 The effect of changes in the distance between the inner fin (solid fin) and the center of the cavity on (**a**) the Nu and the average temperature (**b**) efficiency and effectiveness

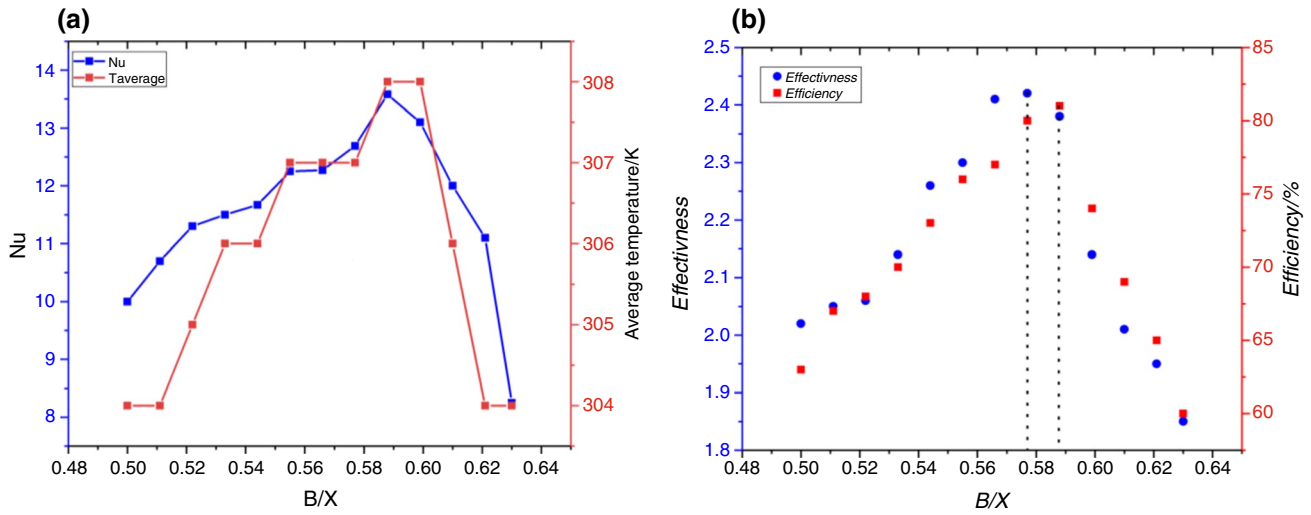

Fig. 7 The effect of changes in the distance between the outer fin and the center of the cavity on (**a**) the Nu and the average temperature (**b**) efficiency and effectiveness

by a decline. An increase in the average temperature also led to an enhancement in the heat transfer rate. As a result, according to Fig. 8a, the Nu follows the same pattern. Similarly, for efficiency and effectiveness, it was observed that the height of the internal fin in a specific range will increase the efficiency and effectiveness. $^{L}/_{Y} = 0.6$ simultaneously led to the highest efficiency and effectiveness.

As mentioned before, fins attached to the base surface can enhance the heat transfer rate in two ways: (1) incrementing heat transfer surface and (2) changing the flow pattern and intensity of created vortexes. These two factors have the optimum situation at optimum values of fins distance from the center of the cavity and fin height. Further increment in A, B, or L, although leading to a higher hear transfer surface, will decline the intensity of the vortexes, hence decrementing the thermal performance of the cavity. Table 4 shows the range of the independent variables based on the optimization of the dependent parameters. Applying these changes in the geometry of the conical cavity, the most optimal parameters can be obtained compared to the simple state (fin-less case).

Accordingly, Fig. 9 compares the estimated Nu of the fin-less and straightforward conical cavity and the cavity equipped with fins from the optimization for different

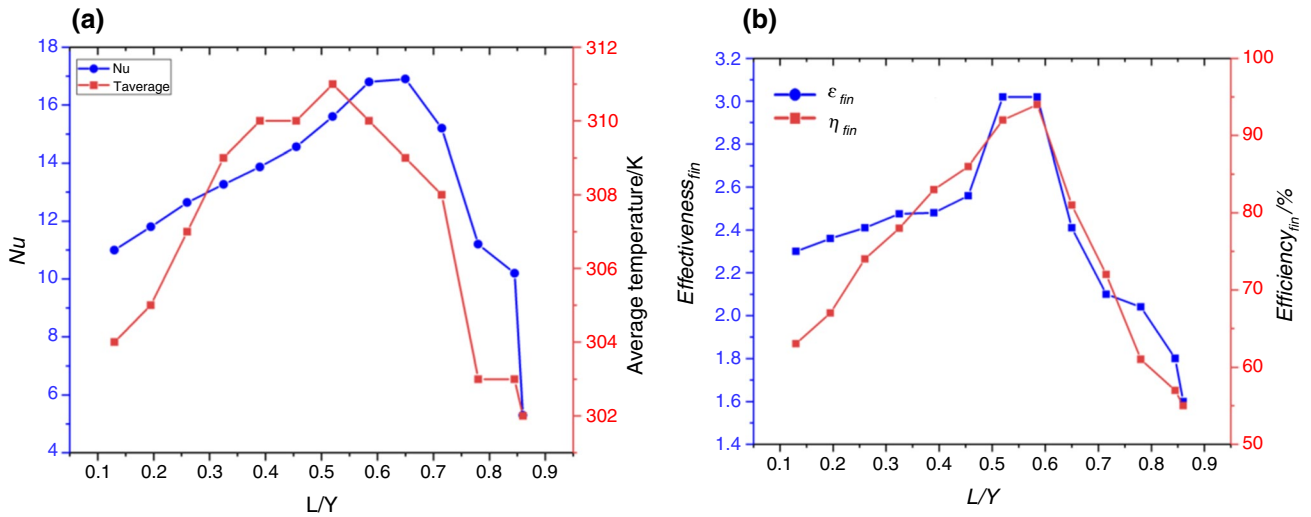

Fig. 8 The effect of changes in the height of the inner on (**a**) the Nu and the average temperature (**b**) efficiency and effectiveness

Table 4 Optimum range of A/X, B/X, and L/Y for different parameters

Parameter	Range		
	Nu	Average temperature	Efficiency and effectiveness
A/X	0.25–0.31	0.23–0.25	0.27–0.31
B/X	0.57–0.62	0.57–0.58	0.57–0.59
L/Y	0.52–0.74	0.48–0.52	0.5–0.6

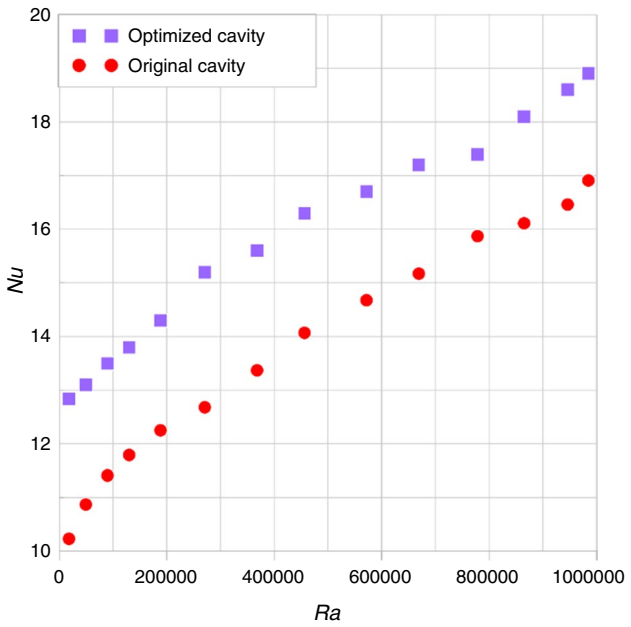

Fig. 9 Comparison of estimated Nu for simple (original cavity) and optimum (optimized cavity) cavities for different Ra

Ra. The results show that the Nu of the optimal cavity is 20.32% higher (the best case) and about 9% higher (the worst case) than the simple one. Figure 9 also suggests that Nu's difference for optimum and simple cavities is more remarkable at lower Ra. In other words, geometric optimization has a more significant effect on low Ra. In the 3D axisymmetric geometry, it is possible to draw a part of geometry by its modeling according to the concept of symmetry which will reduce the computational cost with more focus on the details. Figure 10 is the contour of non-dimensional temperature distribution and streamlines for a section of the optimized and simple conical cavities. The results show that the number and intensity of vortices are higher in the optimized form. The heat transfer surface area also increased upon using fins. The temperature distribution in a simple conical cavity is uniform. The mean temperature also showed a significant increase in the fined state. Another interesting point in Fig. 10 is the displacement of the dominant vortex in the conical cavity. Converting a large vortex to some micro vortices can enhance the heat transfer due to the reduction in the average energy dissipation.

A dimensionless diagram of temperature on the centerline of the conical cavity is plotted in Fig. 11. The dimensionless temperature diagram for the optimized cavity is at most 1.234 times higher than the original case. The important point in Fig. 11 is the behavior of dimensionless temperature profiles along the vertical axis of the conical cavity. By increasing the base surface distance, the temperature changed (i.e. a primary increase, followed by a constant value over a relatively large length). In the highest part of the conical cavity, an increment can be observed in the average temperature. The constant temperature in the middle of the simple cavity can be assigned to a uniform vortex in this region.

Figure 12 shows the velocity contours and vectors of the fluid flow for the two modes. The results indicate a significant alternation in the velocity distribution, inactive vortices in heat transfer and the flow pattern of the optimized form. As mentioned above, any change in the velocity profile leads to variations in temperature distribution.

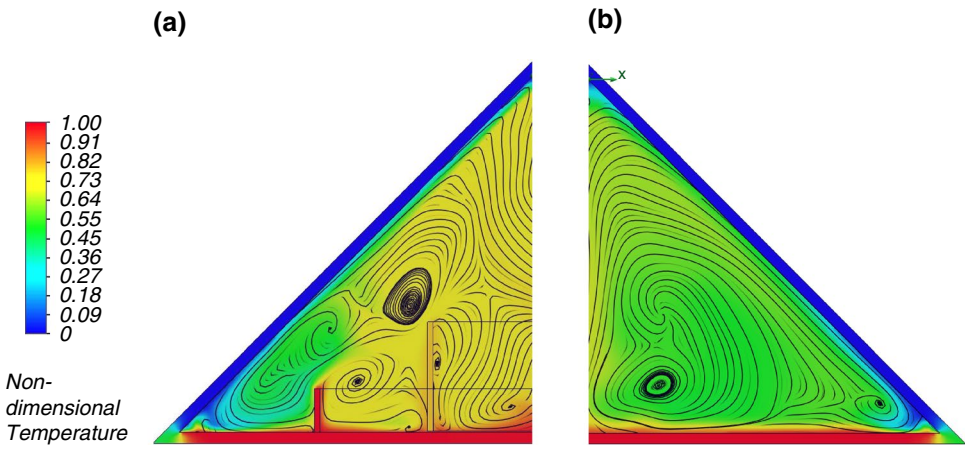

Fig. 10 The non-dimensional temperature contours and streamlines for a section of the **a** optimized and **b** simple mode conical cavities

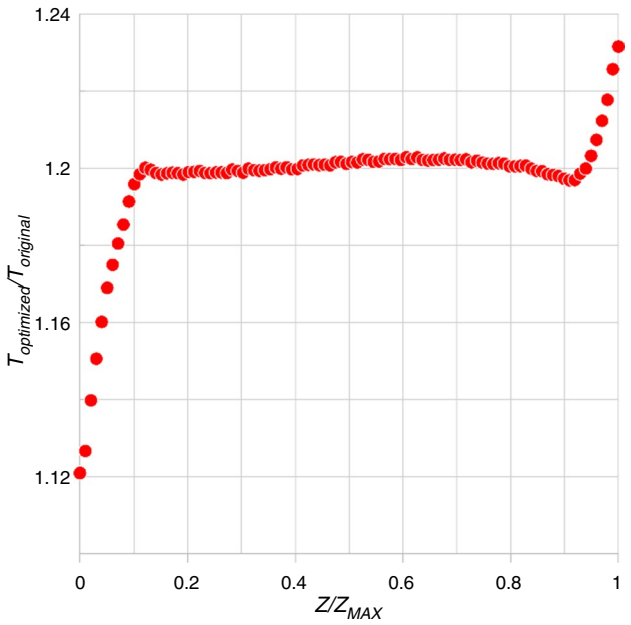

Fig. 11 Dimensionless temperature and vorticity on the centerline of the conical cavity

Porosity optimization

In the former section, the geometric optimization of the inner fins inside the conical cavity was addressed. The results showed that this optimization process could increase the Nu by about 23% in the maximum case. The increase in Nu in the conical cavity can be achieved by changing the internal flow streamlines. The enhancement of the contact surface area has been always one of the significant challenges in heat transfer mechanisms. One of the best ways to increase the contact surface area of a solid body with a fluid (as a two-phase region) is to use a porous medium. By creating porosity on rigid fins, in addition to reducing the thermal inertia caused by the reduction of mass, their contact area with the fluid can be enhanced as well. Based on this, in the continuation of this research, the heat transfer parameters in the conical cavity with the porous fin were investigated. Here, just the inner fin is assumed to be porous. The initial investigations show that the porosity of the outer fin did not significantly affect the cavity performance.

Heat transfer in a porous medium is a combination of convection and conduction mechanisms. The higher the porosity, the greater the fluid–solid contact area. This issue, however, coincides with reducing the cross-sectional area of each element to its adjacent element. In other words, the surface area of convection heat transfer enhances with increasing porosity. But on the other hand, the area used in conduction heat transfer will be reduced. This point will raise the issue of optimal porosity percentage. Any solid object that participates in heat transfer can perform the maximum amount of heat transfer in a range of porosity according to the boundary conditions and the problem assumptions. Another issue of the effect of porosity investigation is the variation of porosity in a specific direction. According to the above explanation, low porosity is desirable for regions where conduction heat transfer needs to be higher (e.g., at the base of the fin). But for regions in which convection heat transfer requires to be higher (e.g., at the tip of the fin), the porosity should be high. In the following sections, the effect of constant and variable porosity will be investigated.

Sensitivity analysis

For optimum fin geometry calculated, the inner fin was assumed at constant porosity. Figure 13 illustrates the Nu, fin efficiency and effectiveness for different porosity of the inner fin at the optimal geometry. As can be seen, the Nu and fin efficiency and effectiveness enhanced followed by a remarkable decline as a function of the porosity percentage.

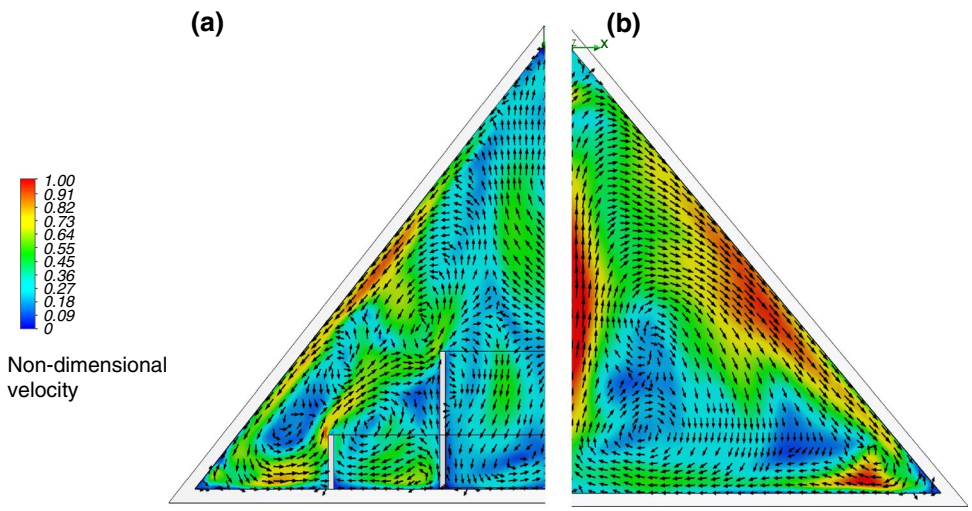

Fig. 12 The non-dimensional velocity contours and velocity vectors for a section of the **a** optimized and **b** simple mode conical cavities

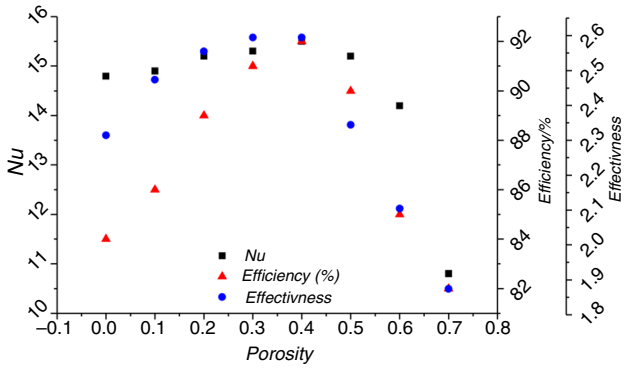

Fig. 13 The effect of changes in the inner fin porosity on the Nu and fin efficiency and effectiveness

The Nu is based on the ratio of convection to conduction heat transfer. According to the previous section, heat transfer in a porous medium was also analyzed in the same manner. Since increasing the porosity percentage enhanced the convection heat transfer coefficient and was associated with a reduction in the area used in conductive heat transfer, at a certain percentage of porosity, the Nu reached a maximum. The thermal efficiency and effectiveness of the fins are similar to the pattern of Nu. As can be seen, all three parameters reach their maximum values at the porosity percentage of ~ 40%. In general, the efficiency and effectiveness of the fin provide a clear definition for heat transfer by defining the surface area in two perspectives, the base area of the fin and the lateral area.

Variable porosity

As seen in the previous section, the porous medium has a drastic effect on the Nu, thermal efficiency, and effectiveness of the fins. It was observed that the temperature decreases along the height of the conical cavity. On the other hand, the internal flow velocities within a conical cavity based on the Ra and Nu reach their maximum values in certain regions. The previous section stated that the amount of porosity is a specific ratio of conduction to convection. In other words, concerning porosity, the amount of convection and conduction can be determined based on the contact area of the fluid with the body. In this section, by adding different porosity percentages, an attempt is made to optimize the functional porosity of fins in the conical cavity by studying the changes in porosity based on the temperature distribution function. The obtained result is used to redesign the percentage and porosity of this environment. In the parts near the base of the conical cavity, the temperature gradient was higher due to its proximity to the heat flux boundary condition and constant high temperature. Due to the strong temperature gradient and flow velocity in the area near the conical cavity base, two views are proposed to change the porosity percentage.

1. *Model#1 (Descending porosity)*: In the first model, porosity can be defined based on velocity changes. The velocity is lower near the base of the conical cavity and the convection heat transfer is small. Higher porosity in this region can improve convection heat transfer by increasing the contact area between the solid surfaces. In the upward direction along the fin, a reduction in the percentage of porosity and the increment in the flow velocity will lead to an appropriate ratio of convection heat transfer due to the interaction between surface area and velocity.
2. *Model#2 (ascending porosity)*: In contrast with the first model, the second view is based on the temperature gradient, the porous medium can be considered in the area near the base of the cavity with less porosity and then the percentage of porosity is gradually increased with height. These changes are based on the theory of increasing heat transfer to higher levels to use the maximum thermal gradient. The relative velocity inside the porosity grows up as the percentage of porosity increases. Consequently, total heat transfer can be improved by increasing the convection heat transfer coefficient (rising the velocity of fluid) and increasing the contact surface area (higher porosity). Due to the low percentage of porosity at the base of the fins in the conical cavity, more heat flux moves along the fin, implying more convection heat transfer in the upper parts and more thermal conductivity in the vicinity of the conical cavity base.

In Fig. 14, two different models (descending and ascending function) of porosity distribution are exhibited along the height of the inner fin. Four functions (constant, linear, and two nonlinear) are considered for each type. These functions are mainly applied based on computational limitations. The equation of porosity along the fin is present in Table 5.

Figure 15 indicates the changes in the Nu based on dimensionless length (height) for two models. The results clearly show that the porosity distribution model had a substantial impact on Nu. For the descending model, function#4 led to the maximum local value for the Nu at the middle of the cavity. For ascending model, function#3 resulted in the highest local Nu at the middle and the cavity base.

Average Nu in the cavity is shown in Fig. 16 for different descending and ascending models. It can be observed that in the descending model, function#3 led to a higher mean Nu; while the highest mean Nu was achieved in the ascending model using function #4.

The interaction between thermal and fluid behavior in a conical cavity determines the final value of the Nu. The higher the vortices' velocity, the more heat is transferred

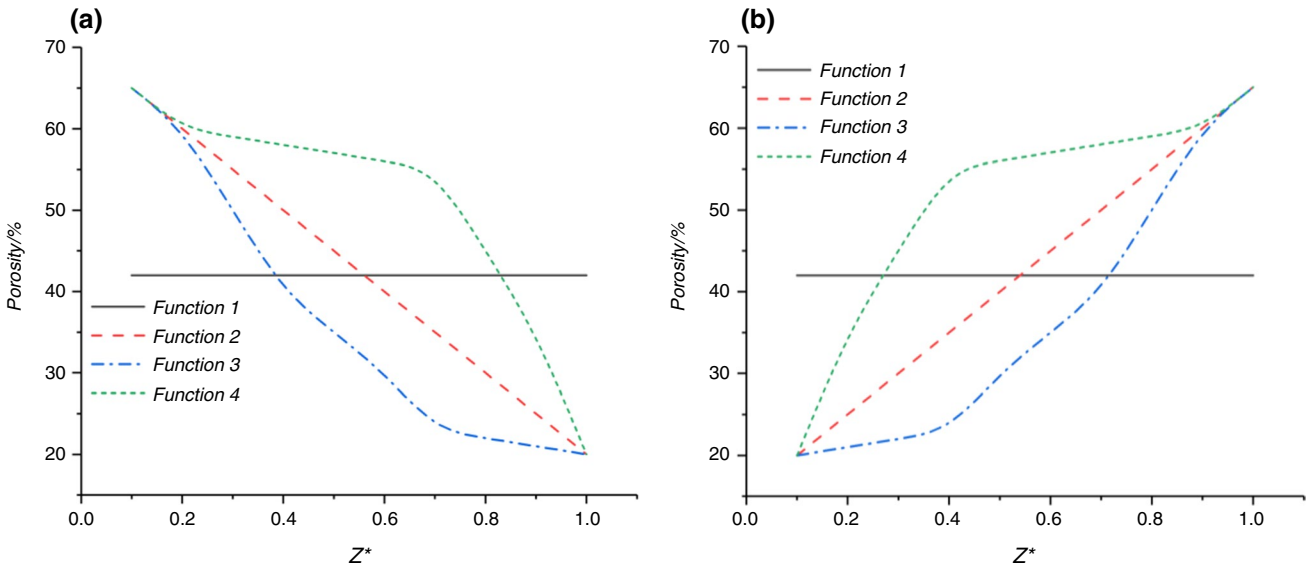

Fig. 14 Two different types of porosity distribution functions **a** model#1 descending and **b** model#2 ascending for the inner fin in the direction of height

Table 5 Variable porosity function

Function	Equation
4	$y = -171.04x^3 + 205.98x^2 - 87.587x + 71.564$ $R^2 = 0.999$
3	$y = 38.304x^3 - 7.6115x^2 - 84.765x + 74.661$ $R^2 = 0.9981$
2	$y = -x$
1	$y = C$

from the hot plate to the fluid according to the geometry of the problem. The temperature distribution changed based on the transfer of the vortices and their heat transfer. An alternation in the porosity percentage along the fin due to the intensity of local vortices and the temperature distribution can affect the Nu. It was observed that the application of descending and ascending porosity models along the fin affects the Nu to some extent. The results showed that eventually, the increased porosity percentage along the inner fin (low porosity near base parts and higher porosity in the upper parts) with function#4 could positively affect the Nu.

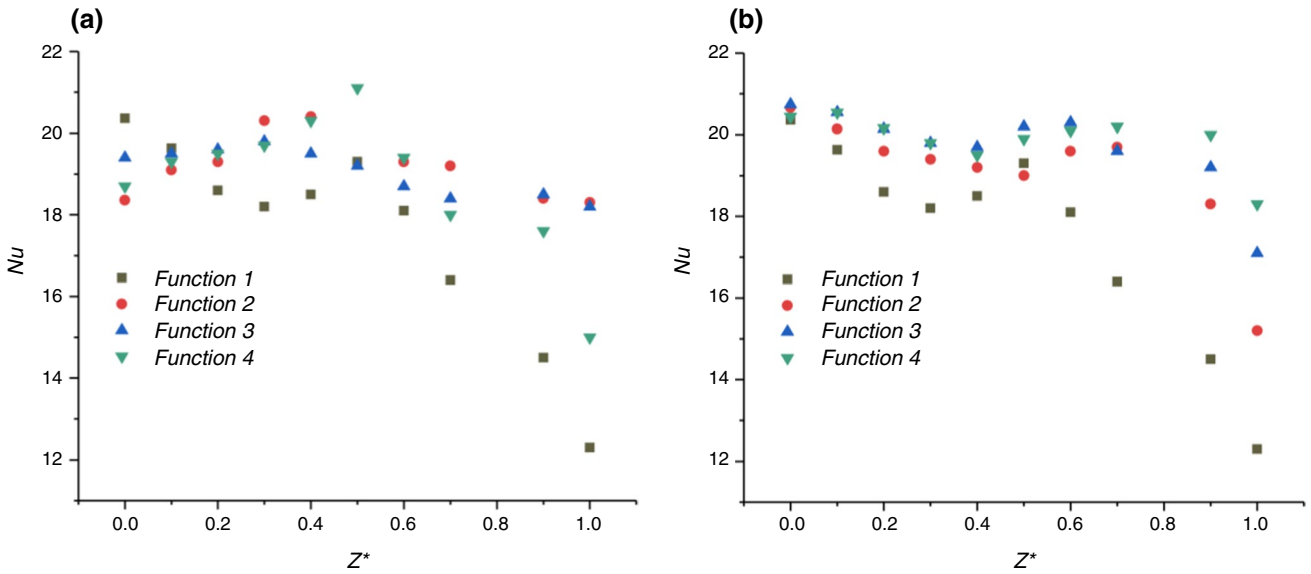

Fig. 15 Variation of local Nu in the direction of cavity height **a** model#1 descending and **b** model#2 ascending

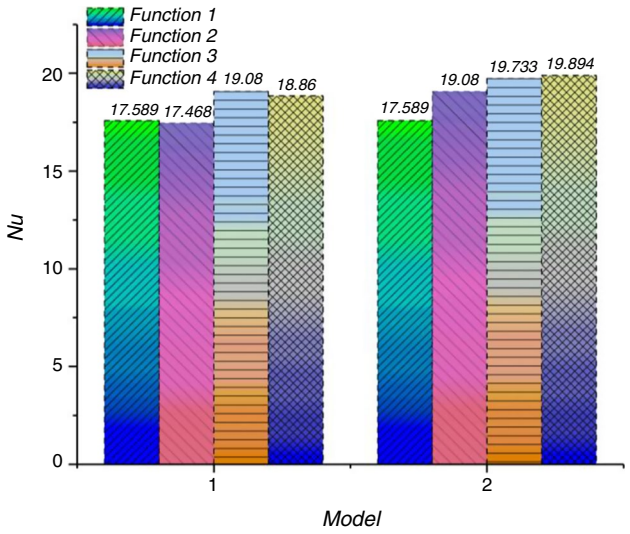

Fig. 16 The average Nu for different models

Conclusions

Conical cavities can be used as concentrators in solar energy absorbers. The better the thermal performance of this cavity, the higher the performance of the solar system. In this work, the thermal performance of the conical cavity was investigated with two concentric cylindrical fins. The effect of the geometric parameters of the fins, including the distance of the inner and outer fins to the center of the cavity and the height of the inner fin, was analyzed. After geometric optimization, the inner fin was considered porous, and the effect of constant and variable porosity was investigated on the thermal performance of the conical cavity. The optimal porosity was obtained in these two cases. The results can be summarized as:

1. The thermal performance of a conical cavity is more sensitive to changes in the height of the inner fin than changes in its distance from the center of the cavity.
2. The best range of inner fin height is 0.48 to 0.74 times the total height of the cone.
3. The best range of the distance from the inner fin to the cone center is 0.23 to 0.31 times the cone base radius.
4. The best range of the distance from the outer fin to the cone center is 0.57 to 0.62 times the cone base radius.
5. The best possible porosity for the inner fin at a constant porosity case is about 40%.
6. The best porosity pattern of the inner fin involves the nonlinear increase in the base porosity to the tip of the cone, in such a way that its increase is more intense near the base and milder near the cone tip.

Acknowledgement The second author acknowledges Postdoctoral Fellowship from KMUTT. The third author acknowledges the support provided by the "Research Chair Grant" National Science and Technology Development Agency (NSTDA), and King Mongkut's University of Technology Thonburi through the "KMUTT 55th Anniversary Commemorative Fund".

References

1. Lovegrove K, Stein W. Concentrating solar power technology: principles, developments and applications. Elsevier; 2012.
2. Reddy K, Vikram TS, Veershetty G. Combined heat loss analysis of solar parabolic dish–modified cavity receiver for superheated steam generation. Sol Energy. 2015;121:78–93.
3. Prakash M. Numerical study of natural convection heat loss from cylindrical solar cavity receivers. IntSchol Res Notices. 2014. https://doi.org/10.1155/2014/104686.
4. Si-Quan Z, Xin-Feng L, Liu D, Qing-Song M. A numerical study on optical and thermodynamic characteristics of a spherical cavity receiver. ApplThermEng. 2019;149:11–21.
5. Liang H, Zhu C, Fan M, You S, Zhang H, Xia J. Study on the thermal performance of a novel cavity receiver for parabolic trough solar collectors. Appl Energy. 2018;222:790–8.
6. Al-Kouz W, Alshare A, Kiwan S, Al-Muhtady A, Alkhalidi A, Saadeh H. Two-dimensional analysis of low-pressure flows in an inclined square cavity with two fins attached to the hot wall. Int J ThermSci. 2018;126:181–93.
7. Ngo L, Bello-Ochende T, Meyer JP. Three-dimensional analysis and numerical optimization of combined natural convection and radiation heat loss in solar cavity receiver with plate fins insert. Energy Convers Manage. 2015;101:757–66.
8. Khanafer K, AlAmiri A, Bull J. Laminar natural convection heat transfer in a differentially heated cavity with a thin porous fin attached to the hot wall. Int J Heat Mass Transf. 2015;87:59–70.
9. Siavashi M, Yousofvand R, Rezanejad S. Nanofluid and porous fins effect on natural convection and entropy generation of flow inside a cavity. Adv Powder Technol. 2018;29(1):142–56.
10. Alshuraiaan B, Khanafer K. The effect of the position of the heated thin porous fin on the laminar natural convection heat transfer in a differentially heated cavity. IntCommun Heat Mass Transfer. 2016;78:190–9.
11. Asl AK, Hossainpour S, Rashidi M, Sheremet MA, Yang Z. Comprehensive investigation of solid and porous fins influence on natural convection in an inclined rectangular enclosure. Int J Heat Mass Transf. 2019;133:729–44.
12. Mesgarpour M, Heydari A, Saedodin S. Comparison of free convection flow around an engineered porous fin with spherical connections and rigid fin under different positioning angles—An experimental and numerical analysis. Phys Fluids. 2019;31(3):037110.
13. Mesgarpour M, Heydari A, Saedodin S. Numerical analysis of heat transfer and fluid flow in the bundle of porous tapered fins. Int J ThermSci. 2019;135:398–409.
14. Daabo AM, Mahmoud S, Al-Dadah RK. The optical efficiency of three different geometries of a small scale cavity receiver for concentrated solar applications. Appl Energy. 2016;179:1081–96.
15. Pérez-Rábago C, Marcos M, Romero M, Estrada C. Heat transfer in a conical cavity calorimeter for measuring thermal power of a point focus concentrator. Sol Energy. 2006;80(11):1434–42.
16. Garrido J, Aichmayer L, Abou-Taouk A, Laumert B. Experimental and numerical performance analyses of a dish-stirling cavity receiver: geometry and operating temperature studies. Sol Energy. 2018;170:913–23.

17. Alsabery AI, Ismael MA, Chamkha AJ, Hashim I. Effect of non-homogeneous nanofluid model on transient natural convection in a non-Darcy porous cavity containing an inner solid body. IntCommun Heat Mass Transfer. 2020;110:104442.
18. Aneja M, Chandra A, Sharma S. Natural convection in a partially heated porous cavity to Casson fluid. IntCommun Heat Mass Transfer. 2020;114:104555.
19. Estellé P, Mahian O, Maré T, Öztop HF. Natural convection of CNT water-based nanofluids in a differentially heated square cavity. J Therm Anal Calorim. 2017;128(3):1765–70.
20. Dogonchi A, Chamkha AJ, Ganji D. A numerical investigation of magneto-hydrodynamic natural convection of Cu–water nanofluid in a wavy cavity using CVFEM. J Therm Anal Calorim. 2019;135(4):2599–611.
21. Dogonchi A, Ismael MA, Chamkha AJ, Ganji D. Numerical analysis of natural convection of Cu–water nanofluid filling triangular cavity with semicircular bottom wall. J Therm Anal Calorim. 2019;135(6):3485–97.
22. Matori A, Mohebbi R, Hashemi Z, Ma Y. Lattice Boltzmann study of multi-walled carbon nanotube (MWCNT)-Fe 3 O 4/water hybrid nanofluids natural convection heat transfer in a Π-shaped cavity equipped by hot obstacle. J Therm Anal Calorim. 2019;136(6):2495–508.
23. Mohebbi R, Mehryan S, Izadi M, Mahian O. Natural convection of hybrid nanofluids inside a partitioned porous cavity for application in solar power plants. J Therm Anal Calorim. 2019;137(5):1719–33.
24. Ghalambaz M, Mehryan S, Izadpanahi E, Chamkha A, Wen D. MHD natural convection of Cu–Al 2 O 3 water hybrid nanofluids in a cavity equally divided into two parts by a vertical flexible partition membrane. J Therm Anal Calorim. 2019;138(2):1723–43.
25. Ghalambaz M, Doostani A, Izadpanahi E, Chamkha AJ. Conjugate natural convection flow of Ag–MgO/water hybrid nanofluid in a square cavity. J Therm Anal Calorim. 2020;139(3):2321–36.
26. Ali FH, Hamzah HK, Egab K, Arıcı M, Shahsavar A. Non-Newtonian nanofluid natural convection in a U-shaped cavity under magnetic field. Int J MechSci. 2020;186:105887.
27. Ramezanizadeh M, Alhuyi NM. Modeling thermal conductivity of Ag/water nanofluid by applying a mathematical correlation and artificial neural network. Int J Low-Carbon Technol. 2019;14(4):468–74. https://doi.org/10.1093/ijlct/ctz030.
28. Komeilibirjandi A, Raffiee AH, Maleki A, AlhuyiNazari M, Safdari SM. Thermal conductivity prediction of nanofluids containing CuO nanoparticles by using correlation and artificial neural network. J Therm Anal Calorim. 2020;139(4):2679–89. https://doi.org/10.1007/s10973-019-08838-w.
29. Maleki A, Elahi M, Assad MEH, AlhuyiNazari M, SafdariShadloo M, Nabipour N. Thermal conductivity modeling of nanofluids with ZnO particles by using approaches based on artificial neural network and MARS. J Therm Anal Calorim. 2020. https://doi.org/10.1007/s10973-020-09373-9.
30. Rostami S, Aghakhani S, HajatzadehPordanjani A, Afrand M, Cheraghian G, Oztop HF, et al. A review on the control parameters of natural convection in different shaped cavities with and without nanofluid. Processes. 2020;8(9):1011.
31. Ho CJ, Chen D-S, Yan W-M, Mahian O. Buoyancy-driven flow of nanofluids in a cavity considering the Ludwig-Soret effect and sedimentation: numerical study and experimental validation. Int J Heat Mass Transf. 2014;77:684–94. https://doi.org/10.1016/j.ijheatmasstransfer.2014.05.059.
32. Safaei MR, Karimipour A, Abdollahi A, Nguyen TK. The investigation of thermal radiation and free convection heat transfer mechanisms of nanofluid inside a shallow cavity by lattice Boltzmann method. Phys A. 2018;509:515–35.
33. Goodarzi H, Akbari OA, Sarafraz MM, Karchegani MM, Safaei MR, Sheikh Shabani GA. Numerical simulation of natural convection heat transfer of nanofluid with Cu, MWCNT, and Al2O3 nanoparticles in a cavity with different aspect ratios. J Thermal SciEngAppl. 2019. https://doi.org/10.1115/1.4043809.
34. Abbassi MA, Safaei MR, Djebali R, Guedri K, Zeghmati B, Alrashed AAAA. LBM simulation of free convection in a nanofluid filled incinerator containing a hot block. Int J MechSci. 2018;144:172–85. https://doi.org/10.1016/j.ijmecsci.2018.05.031.
35. Kolsi L, Mahian O, Öztop HF, Aich W, Borjini MN, Abu-Hamdeh N, et al. 3D buoyancy-induced flow and entropy generation of nanofluid-filled open cavities having adiabatic diamond shaped obstacles. Entrophy. 2016;18(6):232. https://doi.org/10.3390/e18060232.
36. Yousefzadeh S, Rajabi H, Ghajari N, Sarafraz MM, Akbari OA, Goodarzi M. Numerical investigation of mixed convection heat transfer behavior of nanofluid in a cavity with different heat transfer areas. J Therm Anal Calorim. 2020;140(6):2779–803. https://doi.org/10.1007/s10973-019-09018-6.
37. HajatzadehPordanjani A, Aghakhani S, Karimipour A, Afrand M, Goodarzi M. Investigation of free convection heat transfer and entropy generation of nanofluid flow inside a cavity affected by magnetic field and thermal radiation. J Therm Anal Calorim. 2019;137(3):997–1019. https://doi.org/10.1007/s10973-018-7982-4.
38. Ramezanizadeh M, AlhuyiNazari M, Ahmadi MH, Chau K-w. Experimental and numerical analysis of a nanofluidicthermosyphon heat exchanger. EngApplComput Fluid Mech. 2019;13(1):40–7. https://doi.org/10.1080/19942060.2018.1518272.
39. Ghalandari M, Maleki A, Haghighi A, SafdariShadloo M, AlhuyiNazari M, Tlili I. Applications of nanofluids containing carbon nanotubes in solar energy systems: a review. J MolLiq. 2020;313:113476. https://doi.org/10.1016/j.molliq.2020.113476.
40. Ramezanizadeh M, AlhuyiNazari M, Ahmadi MH, Açıkkalp E. Application of nanofluids in thermosyphons: a review. J MolLiq. 2018;272:395–402. https://doi.org/10.1016/j.molliq.2018.09.101.
41 MesgarPour M, Heydari A, Wongwises S. Geometry optimization of double pass solar air heater with helical flow path. Sol Energy. 2012;213:67–80. https://doi.org/10.1016/j.solener.2020.11.015.
42. Tric E, Labrosse G, Betrouni M. A first incursion into the 3D structure of natural convection of air in a differentially heated cubic cavity, from accurate numerical solutions. Int J Heat Mass Transf. 2000;43(21):4043–56.
43. Gorla RSR, Bakier A. Thermal analysis of natural convection and radiation in porous fins. IntCommun Heat Mass Transfer. 2011;38(5):638–45.
44. Mesgarpour M, Heydari A. Numerical investigation of heat transfer in a sintered porous fin in a channel flow with the aim of material determination. Journal of Heat and Mass Transfer Research. 2019;6(1):63–74.
45. Versteeg HK. 1995 An introduction to computational fluid dynamics the finite volume method, 2/E. Pearson Education India; .
46. Yoo D-H, Hong K, Hong T, Eastman J, Yang H-S. 2007 Thermal conductivity of Al2O3/water nanofluids. Journal of the Korean Physical Society.51(1).
47. Esfe MH, Saedodin S, Mahian O, Wongwises S. Thermal conductivity of Al 2 O 3/water nanofluids. J Therm Anal Calorim. 2014;117(2):675–81.
48. Masuda H, Ebata A, Teramae K, Hishinuma N, Ebata Y. 1993 Alteration of thermal conductivity and viscosity of liquid by dispersing ultra-fine particles (dispersion of γ-Al2O3, SiO2 and TiO2 ultra-fine particles). https://doi.org/10.2963/jjtp.7.227
49. Nguyen C, Desgranges F, Galanis N, Roy G, Maré T, Boucher S, et al. Viscosity data for Al2O3–water nanofluid—hysteresis: is heat transfer enhancement using nanofluids reliable? Int J ThermSci. 2008;47(2):103–11.

50. Madavan N, editor. Aerodynamic shape optimization using hybridized differential evolution. 21st AIAA Applied Aerodynamics Conference; 2003.
51 Kaya N. Shape optimization of rubber bushing using differential evolution algorithm. Sci World J. 2014. https://doi.org/10.1155/2014/379196.
52. Price K, Storn RM, 2006 Lampinen JA. Differential evolution: a practical approach to global optimization. Springer Science & Business Media.
53. Chowdhury R, Parvin S, Khan MAH. Finite element analysis of double-diffusive natural convection in a porous triangular enclosure filled with Al2O3-water nanofluid in presence of heat generation. Heliyon. 2016;2(8):e00140.